J. Chem. Sci. Vol. 124, No. 3, May 2012, pp. 557–563. © Indian Academy of Sciences.

Synthesis and characterization of nano silicon and titanium nitride powders using atmospheric microwave plasma technique

S MAHENDRA KUMAR[1], K MURUGAN[2], S B CHANDRASEKHAR[2], NEHA HEBALKAR[2], M KRISHNA[1], B S SATYANARAYANA[1] and GIRIDHAR MADRAS[3,*]
[1]Department of Mechanical Engineering, R V College of Engineering, Mysore Road, Bangalore 560 059, India
[2]Centre for Nanomaterials, International Advanced Research Centre for Powder Metallurgy and New Materials (ARCI), Hyderabad 500 005, India
[3]Department of Chemical Engineering, Indian Institute of Science, Bangalore 560 012, India
e-mail: giridhar@chemeng.iisc.ernet.in

MS received 23 November 2011; revised 21 December 2011; accepted 11 January 2012

Abstract. We have demonstrated a simple, scalable and inexpensive method based on microwave plasma for synthesizing 5 to 10 g/h of nanomaterials. Luminescent nano silicon particles were synthesized by homogenous nucleation of silicon vapour produced by the radial injection of silicon tetrachloride vapour and nano titanium nitride was synthesized by using liquid titanium tetrachloride as the precursor. The synthesized nano silicon and titanium nitride powders were characterized by XRD, XPS, TEM, SEM and BET. The characterization techniques indicated that the synthesized powders were indeed crystalline nanomaterials.

Keywords. Scalable synthesis; microwave plasma; chemical synthesis; nanoparticles.

1. Introduction

Silicon nanoparticles attract a great deal of attention as they are used in logic gates, memory devices, light-emitting devices, sensors, bio-imaging, energy storage and photonic applications.[1] Titanium nitride (TiN) is extensively used as an anti-wear coating,[2] bio replacements,[3] contact/barrier layer to silicon and as a gate electrode in MOS circuits[4,5] due to its high hardness, good conductivity, chemical durability and high melting point.

Several methods have been developed to synthesize crystalline silicon powder on a laboratory (mg/h) scale such as solution routes using a variety of reducing agents,[6–10] microemulsion technique,[11,12] laser ablation,[13,14] mechanochemical synthesis,[15] oxidation of metal silicides[16] and laser-induced pyrolysis of silane.[17] The techniques used for synthesizing nanocrystalline TiN are by heat treatment of the precursor obtained by reacting liquid $TiCl_4$ with NH_3 in anhydrous organic liquids,[18,19] one-pot solvothermal synthesis,[20] carbothermal reduction and nitridation of TiO_2 at high pressure,[21] reacting TiO_2 with sodium amide at low temperature.[22] Microwave plasma heating, self propagating high temperature synthesis[23] and plasma nitridation of metal oxides have also been developed to prepare the transition metal nitride crystals.[24]

Thus, nanoparticle synthesis by 'bottom-up' chemical processing has been extensively used but very few methods are available to produce silicon and titanium nitride nanopowder in the form of particles in large or continuous scale production other than top–down approaches such as mechanical milling.[6] Nanoparticle synthesis in the gas phase is attractive for large and continuous scale production as it does not involve the liquid by-products of wet chemistry processes. The product particles can readily be separated from the gas stream without any post processing, which results in materials of high purity.[18]

Si has been produced by pyrolysis of silane in a microwave plasma reactor[25–27] and from silicon tetrachloride precursor using zinc vapour reduction.[28] Theoretically, gaseous phase reduction of $SiCl_4$ in hydrogen atmosphere is a spontaneous reaction at the room temperature. However, there are practical difficulties in developing a process to cross over the crystallization barrier for the homogeneous nucleation of silicon, as it is extremely difficult to achieve the supersaturation required for homogeneous nucleation.[30]

The microwave plasma technique is ideally suited for rapid evaporation and decomposition of precursor

---

[*] For correspondence

materials, which results in nanoparticles of excellent purity with high production rates.[30–35] In addition, microwave plasma demonstrates good stability, uniform temperature field and can operate at normal ambient pressure.[31] Another advantage of microwave plasma synthesis is the lower reaction temperature as compared to dc or rf plasma and the combined effect of temperature and dielectric heating of precursors.[34]

In this paper, we have demonstrated the synthesis of free flow silicon and titanium nitride nanoparticles on a pilot scale with high production rates (7 g/h). We have developed the technique for the synthesis of Si by using the cheap silicon tetrachloride as the precursor instead of silane as the precursor,[26,27] which is highly pyrophoric. Microwave plasma synthesis method operates at lower reaction temperature and at normal ambient pressure and thus is more economical than conventional processes. Further, the use of $SiCl_4$ as a precursor reduces the cost in this process. We have synthesized TiN using argon as the inert gas, oxygen as the reactive gas and hydrogen as carrier gas. To the best of our knowledge, microwave plasma synthesis of silicon nanopowder by the reduction of a cheap precursor (silicon tetrachloride) has been reported for the first time.

2. Experimental

2.1 *Powder synthesis*

Si and TiN nanopowders were synthesized using the microwave plasma technique (MWP). Figure 1 shows the schematic diagram of the experimental set-up for Si and TiN nanopowder synthesis. The MWP system consists of microwave generator (magnetron 5 kW, 2.45 GHz), a plasmatron (where the microwave gets discharged), a cylindrical reaction chamber, water cooled heat exchanger and powder collection unit. Similar experimental set-ups have been reported elsewhere.[30,35] We have carried out suitable modifications in the set-up used in this study in order to obtain TiN and Si nanopowder, handle the reaction gas mixture of argon and oxygen and to have an effective quenching of the product.

The liquid precursors such as silicon tetrachloride ($SiCl_4$) and titanium tetrachloride ($TiCl_4$) (Aldrich Co.) were used as starting raw materials for synthesis of Si and TiN nanopowders, respectively. The microwave was discharged through a cylindrical quartz tube with nitrogen gas at atmospheric pressure. Hydrogen was used as the carrier gas to feed the gaseous streams of

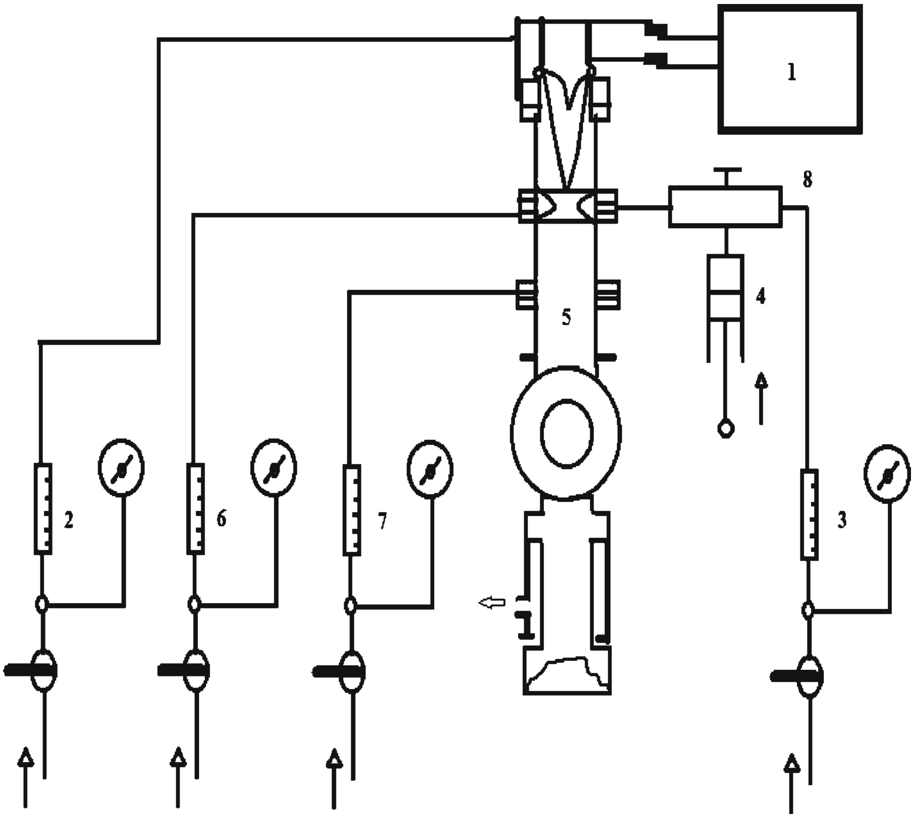

Figure 1. Schematic arrangement of microwave plasma nano particle synthesizing unit. (1) Magnetron; (2) plasma gas flow; (3) carrier gas; (4) $TiCl_4$ feeder; (5) tubular reaction chamber; (6,7) reactive gas; (8) evaporator.

Table 1. Processing parameters for synthesis of Si and TiN nanopowders.

Sl.No	Material synthesized	Flow rate of plasma gas (m^3/h)	Flow rate of carrier gas (m^3/h)	Flow rate of reaction gas (m^3/h)	Operating current (A)	Precursor feeding rate (m^3/h)
1.	Si	2.1	1.3	1.8	1.1	0.8
2.	TiN	2.5	0.6	0.23	1.1	0.6

precursor radially into a tail flame of nitrogen plasma jet in a tubular reaction chamber. The gas mixture of argon and oxygen (96 + 4 vol %) was used with argon as the inert gas and oxygen as a reactive gas for the synthesis of TiN nanopowder. The details of experimental conditions are listed in the table 1.

The liquid precursors were vapourized in the evaporator, were injected uniformly into the plasma chamber and the feeding rate was controlled mechanically. The liquid precursor vapours thermally decompose in the plasma and reacts with nitrogen and other reactants to form the respective nanopowders. These powders were quenched using the water circulated around the reaction chamber and collected in the powder collection drum fitted with filter bag and only powders collected in the filter were used for analysis.

2.2 *Powder characterization*

XRD of the powder was analysed in Bruker AXS D8 diffractometer using Cu-Kα ($\lambda = 15.41874$ nm) radiation to determine the phases present and the crystallite size was determined using the Scherrer formula. The Bragg peaks of the experimental pattern were indexed using ICDD PDF-4 database. The particle shape, size and morphology were analysed using the S4300-N system (Hitachi, Japan) high resolution scanning electron microscope (SEM) and FEI Technai G20 transmission electron microscope (TEM). The surface area and surface chemistry were analysed using Micromeritics' ASAP 2020BET surface area and X-ray photoelectron spectroscopy (XPS), was performed using Omicron X-ray photoelectron spectrometer, respectively.

3. Results and discussion

The microwave plasma technique can be used to control the particle size of the nanomaterial synthesized.[35] Increasing the flow rate of the plasma forming gas and the carrier gas can reduce the average particle size while increasing the feeding rate of precursor materials can increase the average particle size. This is because increasing the flow rate of plasma gas removes the newly formed material in the plasma reaction region, which reduces the residence of these particles leading to a reduction of the particle size.[35] Similarly, the increase of the feeding rate of the raw precursor material increases the concentration of the precursor and the reactive species in the plasma reaction region causing higher particle growth rate. This has been observed for the synthesis of ZrN nanopowders.[35]

3.1 *Formation of nano silicon*

The radially injected gaseous stream of silicon tetrachloride yields homogeneous mixture of gaseous silicon and hydrochloric acid. The possible chemical reactions inside the reaction chamber are

$$\mathrm{SiCl_{4(g)}} + \mathrm{2H_{2(g)}} \leftrightarrow \mathrm{Si_{(s)}} + \mathrm{4HCl_{(g)}}, \tag{1}$$

$$\mathrm{SiCl_{4(g)}} + \mathrm{2H_{2(g)}} \leftrightarrow \mathrm{Si_{(g)}} + \mathrm{4HCl_{(g)}}, \tag{2}$$

$$\mathrm{Si_{(g)}} \leftrightarrow \mathrm{Si_{(s)}}. \tag{3}$$

Reaction 1 shows the crystalline silicon formation from gaseous $SiCl_4$ and hydrogen, which is an endothermic reaction. To make the reaction move forward, continued energy supply is necessary, which would be difficult in a powder synthesizing process; however, this reaction may be suitable for the chemical vapour deposition coating processes, since most CVD reactions are endothermic.[36] Reaction 3 has a negative Gibbs free energy[37] of −400 to −200 kJ/mol when the temperature is increased from 200 to 1400 K. Reaction 2 as a negative Gibbs free energy of −800 to −650 kJ/mol when the temperature is increased from 200 to 1400 K. Reaction 1, however, has a Gibbs free energy that decreases from 200 to 10 kJ/mol when the temperature is increased from 200 to 1400 K. Reaction 2 is a stable spontaneous gas phase reaction and to obtain silicon, both reactions 2 and 3 have to be maintained in the forward direction, which can be accomplished by keeping the partial pressure of the reactants higher compared to the products.

In a simple tubular reaction chamber, maintaining the required partial pressure for the formation of crystalline silicon may not be possible (as it requires removal of enormous amounts of latent heat of vapourization or solidification). Crystallization of silicon from the gaseous phase is, however, possible by providing the required degree of supersaturation.

Assuming the degree of supersaturation is sufficient, particles will nucleate homogeneously.[38] Once nucleation occurs, supersaturation can be relieved by condensation or reaction of the vapour-phase molecules on the resulting particles. Therefore, to prepare small particles, one need to create a high degree of supersaturation, that induces a high nucleation density, followed by immediately quenching the system. Thus, crystalline silicon particles can be obtained by supersaturation of silicon vapour present in the gaseous stream, which can be achieved by quenching the gaseous products in a stream of hydrogen.

3.2 *Effect of quenching gas*

In order to understand the effect of supersaturation on particle formation by homogeneous nucleation, two aspects were considered: quenching and feeding rate (in order to vary the nucleation density). The plasma forming gas (nitrogen) flow rate was fixed at 2.2 m^3/h. Around 40 ml of $SiCl_4$ was fed into the reaction chamber at a rate of 40 and 80 cm^3/min using 1.3 m^3/h of transporting and reducing gas (hydrogen), respectively. Controlled vapour phase feeding of precursor was carried out. To understand the influence of heat removal for the supersaturation of gaseous silicon, hydrogen gas was used as a quenching medium. When there was no quenching gas, nano silicon was not formed even at high precursor feed rates. However, nano silicon was formed with a precursor feed rate of 80 cm^3/min and quenching gas. Thus, it is clear that the required degree of supersaturation for particle formation was possible only with higher precursor feed rate combined with quenching gas. A low feed rate with quenching and without quenching did not yield any particles. In this technique, 3.54 g of silicon nanopowder was synthesized in 30 min, which gives an yield efficiency of 40%.

3.3 *Formation of nano TiN*

In this system, $TiCl_4$ precursor decomposed thermally in the plasma region and reacted with nitrogen radicals to form TiN particles. TiN forms at very high temperatures because of its very low enthalpy of formation and their standard free energies of formation. TiN is formed at temperatures between 1100 and 1600°C at 1 bar nitrogen.[39]

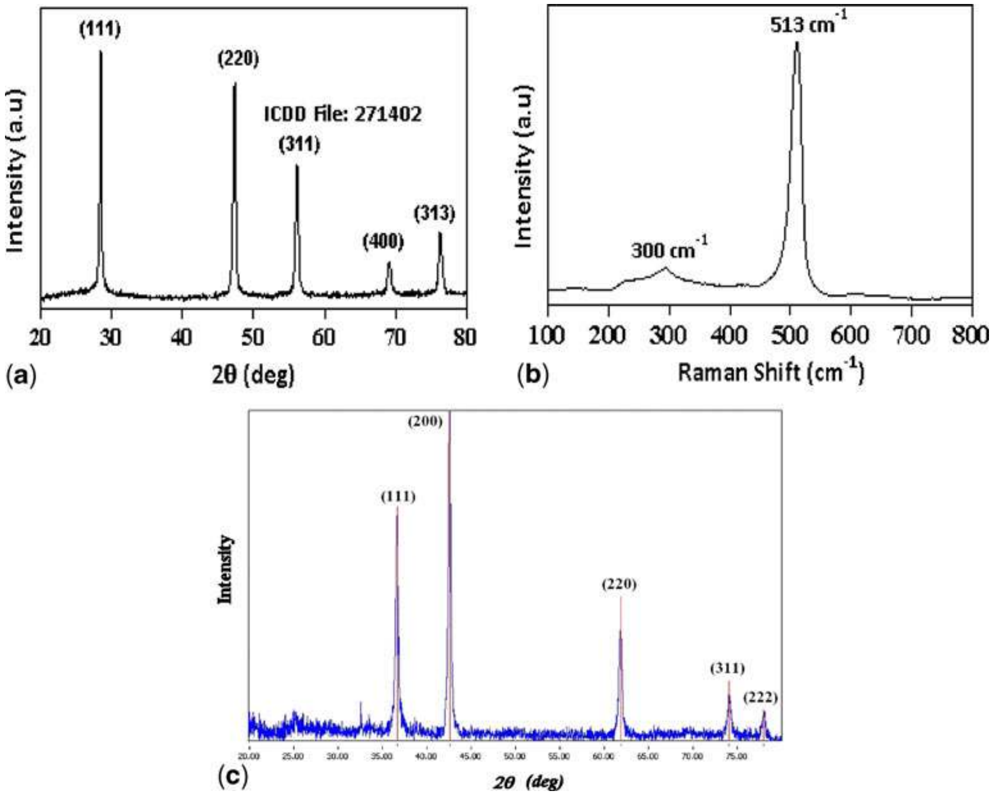

Figure 2. (**a**) XRD pattern of Si nanopowder; (**b**) Raman spectrum of Si; (**c**) XRD of the TiN nanopowder.

4. Structural investigations

4.1 *X-ray diffraction*

The X-ray diffraction analysis was used to determine the crystallinity and the phase of the synthesized compound. Figure 2a shows the XRD pattern of the synthesized Si nanopowder.[40] All the peaks were well-matched with the ICDD file 271402. The average crystallite size estimated, using the Scherrer's equation, from the full width at half maximum (FWHM) of the most intense peak (1 1 1) was 26 nm. Figure 2b is the Raman spectrum of silicon nano powder, which shows a peak at 513 cm^{-1}, which the characteristic peak for nanocrystalline silicon.[41] Since Raman scattering is sensitive to the surface condition of the sample, a small hump at around 300 cm^{-1} was observed in the powder sample,[42] which is attributed to SiO_2 due to a passive layer of SiO_2 formed upon nano Si particles during sample handling.

Figure 2c shows the XRD pattern of the synthesized TiN nanopowder. The patterns show the reflection planes (111), (200), (220), (311), and (222), which indicate the presence of the cubic TiN structure. The average crystallite size of TiN was estimated, using the Scherrer's equation from the full width at half maximum (FWHM) of the most intense peak (200) and was found to be 18 nm.

4.2 *Scanning electron microscopy and transmission electron microscopy*

The SEM and TEM analysis was performed to determine the particle size and morphology of the given powder. Figures 3a and b show the SEM and TEM micrographs of Si nanoparticles. Particle agglomeration is observed in both the micrographs, probably due to the uneven quenching of powder during the process of synthesis. As seen from both the micrographs, the particles

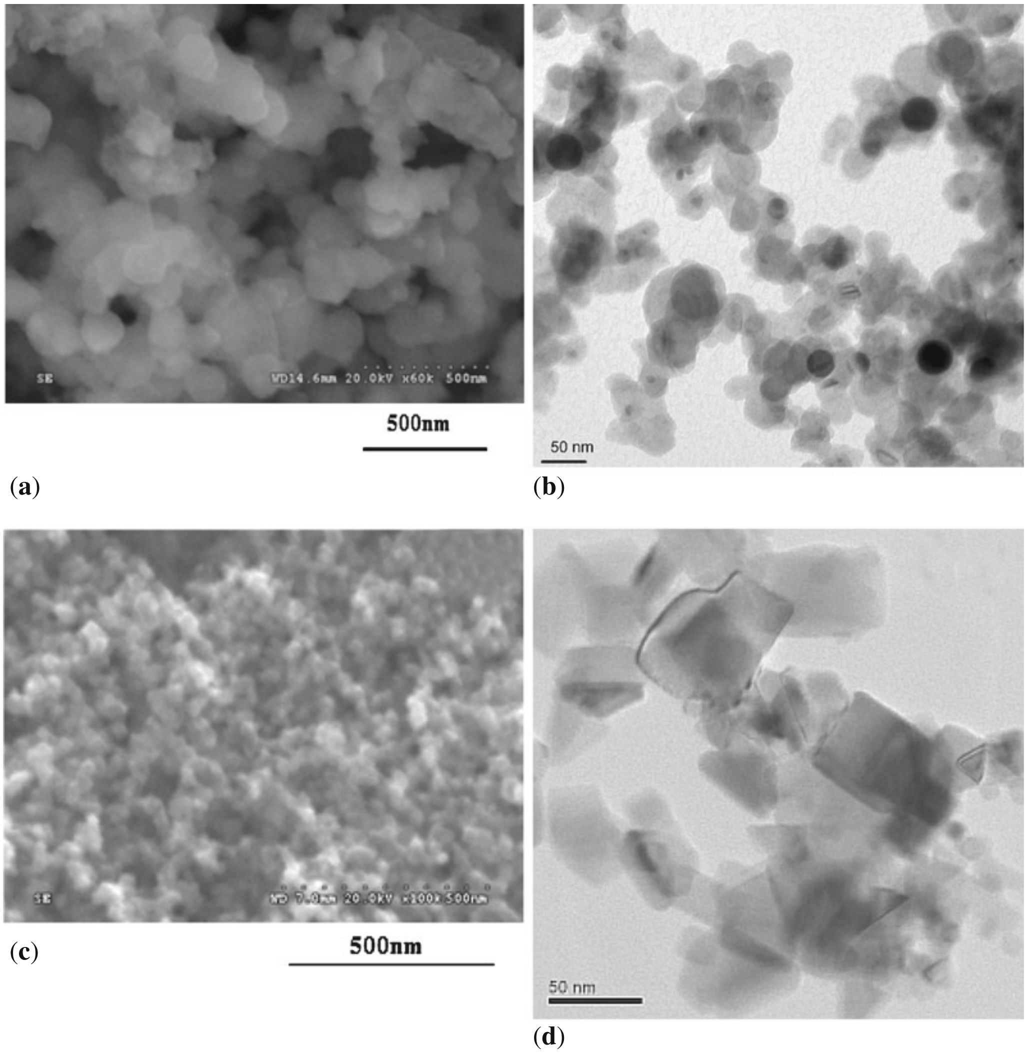

(**a**) (**b**) (**c**) (**d**)

Figure 3. (**a**) SEM and (**b**) TEM micrograph of Si nanopowders. (**c**) SEM and (**d**) TEM micrograph of TiN nanopowders.

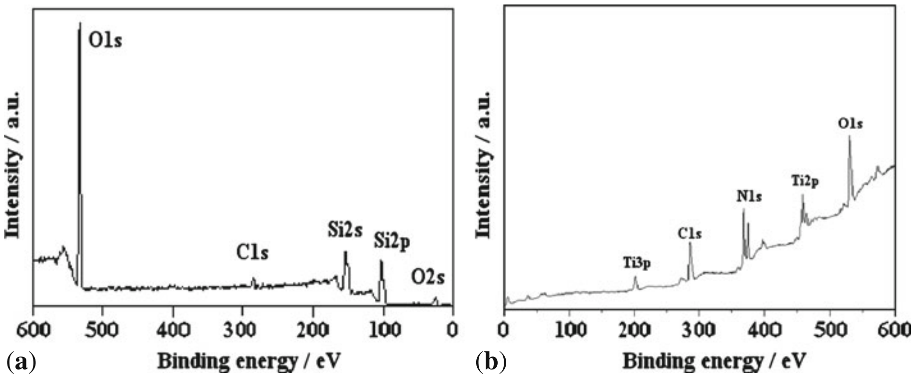

(**a**) (**b**)

Figure 4. XPS spectra of (**a**) Si and (**b**) TiN nanopowder.

are almost spherical and the size of the particle ranges from 20 to 50 nm, which is in good agreement with the crystallite size. Figures 3c and d show the SEM and TEM micrographs of TiN nanoparticles. All the particles are in nanometer range indicating that several particles have formed soft agglomerates. The agglomerates found on the TEM micrographs (figure 3d) is a result of the preparation method for TEM samples and is due to the agglomeration in the liquid film on the TEM grid, which occurs during evaporation of the medium.[43] The BET surface areas of the given Si and TiN nanopowders were found to be 28 and 49 m^2/g, respectively.

4.3 *X-ray photon spectroscopy*

Figures 4a and b show the XPS of the synthesized Si and TiN nanopowders. Figure 4a shows the XPS spectrum of nano silicon particles. The appearance of O peaks indicates the presence of oxide layer on the particle surface. In addition to the binding energy at about 99.066 eV for Si, the distinct Si 2p signal at 102.9 eV is due to the presence of SiO_2 on Si. Figure 4b shows the XPS spectrum of nano TIN particles. The sample surface consists of titanium, nitrogen, oxygen and carbon. The oxygen and carbon peaks in the spectrum are only the surface impurities due to adsorption of CO_2 and oxygen. The N1s spectrum has a peak at 397.2 eV, which corresponds with the Ti2p3/2 and Ti2p1/2 spectra at 458.4 and 464.2 eV indicating the formation of TiN. Quantitative analysis gives Ti:N molar ratio as 1:0.961, which closely agrees with stoichiometric composition of TiN.

5. Conclusions

Silicon nanopowder was successfully synthesized using liquid $SiCl_4$ as the starting raw material by the microwave plasma technique. Considering the precursor cost and yield efficiency, the process may be suitable for the pilot scale production of nano silicon. To improve the conversion efficiency of nano silicon, a high degree of supersaturation should be achieved even at a low precursor feed rate. A highly crystalline titanium nitride nanopowder was also synthesized using the same process. The synthesized Si and TiN had a particle size of about 20 to 50 nm, as determined by SEM and TEM micrographs, respectively. The estimated crystallite size for Si and TiN from XRD were 26 and 18 nm and surface area was found to be 28 and 49 m^2/g, respectively.

Acknowledgements

SMK greatfully acknowledges Dr. G Sundararajan, Director International Advanced Research Centre for Powder Metallurgy and New Materials (ARCI), Hyderabad for permitting to conduct experimental work in his organization and Prof. Krupashankara, Department of Mechanical Engineering, RV College of Engineering, Bangalore for his guidance during experimental work and the management of RV college of Engineering, Bangalore for their continuous support.

References

1. Walters R J, van Loon R V A, Brunets I, Schmitz J and Polman A 2009 *Nat. Mater.* **9** 21
2. Bull S J, Sharkeev Y P, Fortuna S V, Shulepov I A and Perry A J 2011 *J. Mater. Res.* **16** 3293
3. Mändl S 2002 *Surface Coatings Technol.* **156** 276
4. Fillot F, Morel T, Minoret S, Matko I, Maitrejean S, Guillaumot B, Chenevier B and Billon T 2005 *Microelectronic Eng.* **82** 248
5. Kim K S, Jang Y C, Kim K J, Lee N E, Youn S P, Roh K J and Roh Y H 2001 *J. Vacuum Sci. Technol. A: Vacuum, Surfaces, Films* **19** 1164
6. Jakubowicz J, Smardz K and Smardz L 2007 *Physica E* **38** 139

7. Baldwin R K, Pettigrew K A, Ratai E, Augustine M P and Kauzlarich S M 2002 *Chem. Commun.* 1822
8. Neiner D, Chiu H W and Kauzlarich S M 2006 *J. Am. Chem. Soc*. **128** 11016
9. Zhang X, Neiner D, Wang S, Louie A Y and Kauzlarich S M 2007 *Nanotechnology* **18** 095601
10. Bley R A and Kauzlarich S M 1996 *J. Am. Chem. Soc*. **118** 12461
11. Wilcoxon J, Samara G and Provencio P 1999 *Phys. Rev. B* **60** 2704
12. Tilley R D, Warner J H, Yamamoto K, Matsui I and Fujimori H 2005 *Chem. Commun.* 1833
13. Riabinina D, Durand C, Chaker M and Rosei F 2006 *Appl. Phys. Lett*. **88** 073105
14. Svrček V, Sasaki T, Shimizu Y and Koshizaki N 2006 *Appl. Phys. Lett*. **89** 213113
15. Heintz A S, Fink M J and Mitchell B S 2007 *Adv. Mater.* **19** 3984
16. Pettigrew K A, Liu Q, Power P P and Kauzlarich S M 2003 *Chem. Mater*. **15** 4005
17. Li X, He Y, Talukdar S S and Swihart M T 2003 *Langmuir* **19** 8490
18. Pratsinis S and Vemury S 1996 *Powder Technol*. **88** 267
19. Choi D and Kumta P N 2005 *J. Am. Ceram. Soc*. **88** 2030
20. Hu J, Lu Q, Tang K, Yu S, Qian Y, Zhou G and Liu X 2004 *J. Am. Ceram. Soc*. **83** 430
21. Peelamedu R D, Fleming M, Agrawal D K and Roy R 2004 *J. Am. Ceram. Soc*. **85** 117
22. Huang Y, Gu Y, Zheng M, Xu Z, Zeng W and Liu Y 2007 *Mater. Lett*. **61** 1056
23. Yi H C and Moore J J 1990 *J. Mater. Sci*. **25(2)** 1159–1668
24. Vaidhyanathan B and Rao K J 1997 *Chem. Mater*. **9** 1196
25. Gupta A, Swihart M T and Wiggers H 2009 *Adv. Funct. Mater.* **19** 696
26. Knipping J, Wiggers H, Rellinghaus B, Roth P, Konjhodzic D and Meier C 2004 *J. Nanosci. Nanotechnol*. **4(8)** 1039
27. Grimm H, Petermann N, Gupta A and Wiggers H 2010 Synthesis of highly doped silicon and germanium nanoparticles in a low-pressure plasma-reactor for thermoelectric and solar applications. In: *Technical Proceedings of the 2010 NSTI Nanotechnology Conference*. Anaheim, CA 94526, USA, pp 410–412
28. Uesawa N, Inasawa S, Tsuji Y and Yamaguchi Y 2010 *J. Phys. Chem. C* **114** 4291
29. Liu X Y 2000 *J. Chem. Phys*. **112** 9949
30. Kurkin E D I, Troitsky V and Berestenko V 2006 Microwave plasma chemical unit for producing nanopowders. In: Y.A. Lebedev (ed) *IV International Workshop on Microwave Discharges Fundamentals and Application*. Moscow, pp 339–342
31. Chau J, Hsu M, Hsieh C and Kao C 2005 *Mater. Lett*. **59** 905
32. Chau J, Hsu M and Kao C 2006 *Mater. Lett*. **60** 947
33. Chau J L H and Kao C C 2009 *J. Non-Crystalline Solids* **355** 2448
34. Chau J 2007 *Mater. Lett*. **61** 2753
35. Chau J and Kao C 2007 *Mater. Lett*. **61** 1583
36. Choy K 2003 *Prog. Mater. Sci.* **48** 57
37. Lide D R and Frederikse H P R 2000 *C R C Handbook of chemistry and physics*, 78th ed. (Boca Raton, FL: CRC Press) 5.1–5.113
38. Reddy R G 2003 *Rev. Adv. Mater. Sci.* **5(2)** 121
39. Glasson D R and Jayaweera S A A 1968 *J. Appl. Chem*. **18** 65
40. Tong L and Reddy R G 2006 *JOM* **58(4)** 62
41. Verhey J, Bismayer U, Guttler B and Lundt H 1994 *Semiconductor Sci. Technol*. **9** 404
42. Hemley R, Mao H, Bell P and Mysen B 1986 *Phys. Rev. Lett*. **57** 747
43. Dekker J P, van der Put P J, Veringa H J and Schoonman J 1994 *J. Mater. Chem*. **4** 689